

**Structure refinement and new crystal-chemical data for tiragalloite (Mn²⁺_{3.86}Ca_{0.10})_{Σ3.96}(As⁵⁺_{0.85}V⁵⁺_{0.02}Si_{0.19})_{Σ1.06} Si₃O₁₂(OH) from the Scerscen glacier, Val Malenco, Italy**Athos Maria Callegari ^{1,*}, Massimo Boiocchi ², Michele Zema ^{1,3},
Serena Chiara Tarantino ^{1,3}¹ Department of Earth and Environment Sciences, University of Pavia, via Ferrata 1, I-27100 Pavia, Italy² Centre for Scientific Instrumentation, University of Pavia, via Bassi 21, I-27100 Pavia, Italy³ CNR-IGG, via Ferrata 1, I-27100 Pavia, Italy**ARTICLE INFO**

Submitted: June 2019

Accepted: January 2020

Available on line: March 2020

* Corresponding author:
athosmaria.callegari@unipv.it

DOI: 10.2451/2020PM900

How to cite this article:
Callegari A.M. et al. (2020)
Period. Mineral. 89, 77-87**ABSTRACT**

A new sample of tiragalloite from the Scerscen Glacier of the Malenco valley (Lombardy, Italy) has been studied by single-crystal X-ray diffraction and microchemical analyses. Structure refinement in space group $P2_1/n$ converge to $R_1=0.0373$ for 6149 reflections with $I \geq 2\sigma(I)$ and 0.0583 for all 8242 data. The refined unit-cell parameters are: $a=6.6702(2)$ Å, $b=19.9336(7)$ Å, $c=7.5759(2)$ Å, $\beta=95.518(1)^\circ$, $V=1002.63(5)$ Å³, and the crystal-chemical formula is $(\text{Mn}^{2+}_{3.86}\text{Ca}_{0.10})_{\Sigma 3.96}(\text{As}^{5+}_{0.85}\text{V}^{5+}_{0.02}\text{Si}_{0.19})_{\Sigma 1.06}\text{Si}_3\text{O}_{12}(\text{OH})$, with $Z=4$.

The new data of tiragalloite from Scerscen confirm the general organization of the crystal structure, as previously reported in literature for two samples from Graveglia valley, Liguria, Italy, which contained a different amount of V⁵⁺ or As⁵⁺ cations. However, refinement of the site populations at the Mn(3) and Mn(4) sites suggests that the distribution of Ca among these atom sites might be different than that reported in literature. In particular, in tiragalloite from Scerscen, Ca seems to be preferentially located at the ^[6]Mn(4)(O₅OH) octahedron rather than within the large ^[7]Mn(3)O₇ polyhedron. The topology of the $[\text{AsSi}_3\text{O}_{12}(\text{OH})]^{8-}$ unit of tiragalloite is compared with natural and synthetic phases containing similar groups of four tetrahedra.

Keywords: tiragalloite; crystal chemistry; sorosilicates; Malenco valley; Lower Scerscen Glacier.

INTRODUCTION

Tiragalloite, ideally Mn₄AsSi₃O₁₂(OH), is a member of the 57.02 group: “Sorosilicate Insular Si₃O₁₀ and Larger Noncyclic Groups with (Si₄O₁₃) groups” following the Dana type (Gaines et al., 1997), and is a member of the 17.7 group: “Silicates with vanadate, arsenate or antimonate” following the Hey’s Chemical Index of Minerals (Clark, 1993). Tiragalloite from the type locality (Molinello mine, Graveglia valley, Ne village, Genoa province, Liguria, Italy) was discovered and approved as a new specie in 1979 (Gramaccioli et al., 1980). It was named after Paolo Onofrio Tiragallo (1905-1987), a distinguished

amateur mineralogist and curator of the mineralogical collection of the University of Genoa. Tiragalloite was also found in other Italian localities: Lombardy (Sondrio province; Callegari et al., 1992); Aosta Valley (Saint Marcel village; Cenki-Tok and Chopin, 2006); Piedmont (Cuneo and Torino provinces; Piccoli et al., 2007). The mineral was also found in Austria (east and north Tyrol; Abrecht, 1990; Niedermayr et al., 2015), Switzerland (Grisons; Brugger et al., 2006; Roth and Meisser, 2011) and Japan (Kyushu Region; Nakao et al., 2005). For several of these occurrences, chemical data are available (Table 1). However, only three crystallographic studies

are reported in literature, and regard tiragalloite samples from Liguria region: two from the type locality Molinello mine (Gramaccioli et al., 1979, 1980), and one from the Gambatesa mine, located close to the former locality (Nagashima and Armbruster, 2010).

Callegari et al. (1992) reported preliminary data about the occurrence of tiragalloite samples from Malenco valley, Italy, and the chemical characterization of these samples revealed a V depletion coupled with an As enrichment with respect to the type material. In addition, the unit-cell parameters reported in Callegari et al. (1992) were significantly different from those reported in Gramaccioli et al. (1979), in particular as regard the *c* parameter.

This work reports the complete crystal-chemical study of tiragalloite from Malenco valley by combining the results of microchemical and single-crystal X-ray diffraction analyses.

EXPERIMENTAL

Sample

The sample of tiragalloite used in this work comes from metacherts at Vedretta di Scerscen Inferiore, Lower

Scerscen Glacier (Italy) and was provided to the mineral collection of the Museum of Mineralogy of the University of Pavia by Franco Benetti. The sample consists of few isolated anhedral orange crystals, lesser than 1 mm in size. A crystal has been cut to obtain a suitable prismatic single crystal for X-ray diffraction and another fragment was used for chemical analysis.

Chemical data

Preliminary qualitative chemical analyses were performed by energy-dispersive spectrometry (EDS) on a TESCAN FE-SEM (Mira3 XMU-series), coupled with an EDAX APOLLO SDD system at the “Laboratorio Arvedi”, University of Pavia, with the following operative conditions: accelerating voltage 20 kV, beam current ~40 nA, counting time=100 s. The EDS analysis showed that Mn, Si, As, Ca and V were the only elements identified above the detection limit of $Z \geq 8$. Quantitative chemical data were obtained through wavelength-dispersive spectrometry (WDS) mode using a Superprobe JEOL JXA 8200 at the “electron microprobe laboratory” of the University of Milan, using the following analytical

Table 1. Comparison of chemical composition of tiragalloite from several localities.

	1 wt% (e.s.d.)	1 range	2 wt. %	3 wt. %	4 wt. %	5 wt. %	6 wt. %	7 wt. %	8 wt. %
As ₂ O ₅	16.71(22)	16.35-16.94	16.07	12.85	16.91	18.35	16.06	17.83	14.95
V ₂ O ₅	0.28(3)	0.24-0.33	1.67	1.35	0.59	n.d.	0.85	0.0	1.63
Sb ₂ O ₅	-		n.d.*	n.d.	0.01	n.d.	n.d.	n.d.	n.d.
SiO ₂	32.93(19)	32.71-33.29	32.38	35.04	31.45	31.91	31.20	31.58	32.68
TiO ₂	-		n.d.	0.02	n.d.	0.02	<0.05	n.d.	n.d.
Al ₂ O ₃	-		n.d.	0.01	n.d.	0.02	<0.05	n.d.	n.d.
FeO	-		0.17	-	-	0.56	0.17	n.d.	n.d.
MnO	47.05(19)	46.84-47.32	48.34	47.78	46.88	46.02	47.70	47.42	47.20
CaO	0.99(5)	0.93-1.07	0.75	1.12	0.27	0.75	0.63	0.92	1.25
MgO	-		n.d.	-	0.39	0.0	0.21	n.d.	n.d.
PbO	-		n.d.	n.d.	0.04	n.d.	n.d.	n.d.	n.d.
SO ₃	-		n.d.	n.d.	0.03	n.d.	n.d.	n.d.	n.d.
Na ₂ O	-		n.d.	0.01	0.01	0.03	<0.05	n.d.	n.d.
NiO	-		n.d.	0.01	n.d.	n.d.	n.d.	n.d.	n.d.
CuO	-		n.d.	0.03	n.d.	n.d.	n.d.	n.d.	n.d.
K ₂ O	-		n.d.	-	n.d.	<0.01	n.d.	n.d.	n.d.
H ₂ O _{calc}	1.55			2.02					
F	-		n.d.	n.d.	0.11	n.d.	n.d.	n.d.	n.d.
O=F					0.05				
Total	99.51		99.38	100.24	96.59	97.67	96.81	97.75	97.69

1 - This work; 2 - Molinello mine, Italy (Gramaccioli et al., 1980); 3 - Gambatesa, Italy (Nagashima and Armbruster, 2010); 4 - Valletta mine, Italy (Cámara et al., 2015); 5 - Ködnitz Valley, Austria (Abrecht, 1990); 6 - Praborna mine, Italy (Cenki-Tok and Chopin, 2006); 7, 8 - Yamato mine, Japan (Nakao et al., 2005). * n.d. - not detected.

conditions: accelerating voltage 15 kV, beam current 5 nA, nominal beam size 3 μm . Standards (element-emission line) were: rhodonite (Mn-K α), nickeline (As-L α), vanadium (V-K α), and grossular (Si-K α , Ca-K α). Counting times of 30 s on the peak and 10 s on the backgrounds were applied for all the elements. The $\phi(\rho z)$ routine was applied for the correction of the recorded raw data. The occurrence of H₂O as (OH)⁻ groups is suggested by the crystal-structure refinement.

The chemical composition of tiragalloite from Scerscen valley is reported in Table 1, together with the analyses of tiragalloite from other localities for a comparison. The average of the 5 spot analyses were processed in order to give a chemical formula based on 13 oxygen atoms and considering a stoichiometric water content of 1 (OH) group per formula unit (p.f.u.). The minor V content was considered as V⁵⁺ and assumed as a substituent for As⁵⁺ at the tetrahedral site. The resulting empirical formula is $(\text{Mn}^{2+}_{3.86}\text{Ca}_{0.10})_{\Sigma 3.96}(\text{As}^{5+}_{0.85}\text{V}^{5+}_{0.02}\text{Si}_{0.19})_{\Sigma 1.06}\text{Si}_3\text{O}_{12}(\text{OH})$.

X-ray crystallography

Diffraction data up to a resolution of $\sin\theta/\lambda=0.995 \text{ \AA}^{-1}$ ($\theta_{\text{max}}=45^\circ$ for MoK α X-radiation) were collected by means of a Bruker AXS three-circle diffractometer, equipped with the Smart-Apex CCD detector, working at ambient temperature with graphite-monochromated MoK α X-ray radiation. Details of data collection are reported in Table 2. Omega-rotation frames were processed by the SAINT+ software (Bruker, 2003) for data reduction, including background, Lorentz and polarization effects corrections. The semi-empirical absorption correction of Blessing (1995), based on the determination of transmission factors for equivalent reflections, was applied using the program SADABS (Sheldrick, 2003). Unit-cell parameters were obtained by least-square refinement from the positions of 3938 reflections with $I > 10\sigma(I)$ collected in the θ range 3–38°.

The refinement of the structure was performed on F^2 using weighted full-matrix least-squares procedures (SHELXL-2014/7; Sheldrick, 2015), starting from the atomic coordinates given by Nagashima and Armbruster (2010) and using the same site labelling scheme. Being the scattering curve for As⁵⁺ not available in the *International Tables for X-ray Crystallography, Volume C* (Ibers and Hamilton, 1992), for internal consistency, scattering curves for neutral atoms were used for all atoms.

Anisotropic displacement parameters were refined for all non-H atoms. In the first stages of the structure refinement, mean atomic numbers at all cation sites were determined by refining the site occupancies of the main atomic species vs. vacancy. Structure refinement gave occupancy values close to 1 for Mn at the Mn(1) and

Mn(2) sites and slightly lower than 1 at Mn(3) and Mn(4). T(1,2,3) sites resulted to be almost fully occupied by Si, whereas an occupancy value significantly lower than 1 was obtained for As at the T(4) site. Therefore, Mn(1) and Mn(2) sites were considered as fully occupied by Mn, whereas partial substitution of Ca for Mn was allowed at Mn(3) and Mn(4) sites, with the sum of Ca occupancies in the two sites constrained to the Ca content as determined by microchemical analysis within 1 e.s.d. Analogously, the tetrahedrally coordinated T(1), T(2) and T(3) sites were considered as fully occupied by Si, whereas partial substitution of Si for As was allowed at the T(4) site. All sites were considered as fully occupied (sum of site occupancies constrained to 1). The small amount of V detected by microchemical analysis was not considered in the structure refinement.

Table 2. Crystal data and details of structure refinement.

Crystal size (mm)	0.10×0.04×0.02
<i>a</i> (Å)	6.6702(2)
<i>b</i> (Å)	19.9336(7)
<i>c</i> (Å)	7.5759(2)
β (°)	95.518(1)
Volume (Å ³)	1002.63(5)
<i>Z</i>	4
Space group	$P2_1/n$
Wavelength MoK α (Å)	0.7107
Absorption coefficient (mm ⁻¹)	8.34
Sample-to-detector distance (mm)	50
Scan mode	ω
Scan width (°)	0.3
Acquisition times (s)*	20–40
Collected reflections	40972
Unique reflections	8242
Reflections with $I \geq 2\sigma(I)$	6149
R_{int}	0.065
θ range (°)	2–45
<i>h</i> range	-13–13
<i>k</i> range	-39–38
<i>l</i> range	-15–15
Completeness (%)	99.6
F_{000} (e^-)	1112.5
Largest diff. peak / hole ($e^- \text{ \AA}^{-3}$)	1.95/–0.92
R_1 / wR_2 ($I \geq 2\sigma(I)$)	0.037/0.078
R_1 / wR_2 (all data)	0.058/0.087
Gof	0.989

* Two different acquisition times were selected for the two different 2 θ positions of the CCD detector.

After converging of the least-square procedures, the H atom was added to the model in the position reported by Nagashima and Armbruster (2010), which was also located in the ΔF map, and refined assuming a mixed model on atom coordinates. The X-O-H bond angle was constrained to 109.5° , whereas the O-H distance was restrained to $0.98 \pm 0.01 \text{ \AA}$ (Franks, 1973), a values commonly used for minerals and corresponding to the O-H bond length derived from neutron-diffraction data. The restraint is put on the O-H distance only, and the H atom position is free to seek its optimal position around the O atom. The H atom was refined with isotropic displacement parameter constrained to 1.5 times the isotropic equivalent displacement parameter of the oxygen atom of the hydroxyl group.

The final structure refinement converged to final R_1 factors of 0.0373 for 6149 reflections with $I/\sigma(I) \geq 2$ and 0.0583 for all 8242 reflections. The final ΔF map showed a highest peak of $1.95 \text{ e}^-/\text{\AA}^3$ at 0.03 \AA from T(4) site and a maximum hole of $-0.92 \text{ e}^-/\text{\AA}^3$ at 0.92 \AA from the same site. These residuals were ascribed to unaccounted systematic problems with the experimental data and were considered as featureless with respect to the crystallographic results.

Atomic coordinates, site occupancies and equivalent isotropic displacement parameters are listed in Table 3; interatomic distances and other selected geometrical and distortion parameters are compiled in Table 4, while anisotropic displacement parameters are reported in Table 5.

DESCRIPTION OF THE CRYSTAL STRUCTURE

The structure of tiragalloite contains eight crystallographically unique non-H cation sites. Mn atoms at Mn(1) and Mn(2) sites are 6-fold coordinated by oxygen atoms and arranged in octahedral geometry. Mn/Ca atoms at Mn(4) site are coordinated by 5 oxygen atoms and an OH group, also arranged in octahedral geometry. Mn/Ca atoms at Mn(3) are 7-fold coordinated by oxygen atoms and arranged in a distorted geometry for the presence of two long bond distances. Si atom at T(1), T(2), T(3) sites as well as As/Si atoms at T(4) site are 4-fold coordinated in tetrahedral geometries. While coordination around T(1), T(2) and T(4) is ensured by 4 oxygen atoms, Si coordination at T(3) includes one OH group, thus originating a $^{[4]}\text{T}(3)(\text{O}_3\text{OH})$ tetrahedron containing one Si-OH silanol group. Mean $\langle \text{T}(4)\text{-O} \rangle$ bond distance ($1.687(1) \text{ \AA}$) is longer than the other $\langle \text{T-O} \rangle$ distances ($1.629(1)$, $1.623(1)$ and $1.631(1) \text{ \AA}$ for T(1), T(2) and T(3) sites, respectively) because of the presence of As populating the site.

There are thirteen anion sites in the structure of tiragalloite: oxygen atoms at O(6), O(9) and O(12) are 4-fold coordinated, whereas oxygen atoms at the remaining

sites are 3-fold coordinated. The O(11) site hosts the oxygen of the OH group and is bonded to the Mn(4) and T(3) sites, originating the $^{[6]}\text{Mn}(4)(\text{O}_5\text{OH})$ octahedron and the $^{[4]}\text{T}(3)(\text{O}_3\text{OH})$ tetrahedron already described above. The hydroxyl group at O(11) site originates a hydrogen-bond interaction and the geometrical features of the O(11)-H \cdots O(1) hydrogen bond are reported in Table 4.

Wavy ribbons extending along b of edge-sharing 6- and 7-fold coordinated polyhedra, hosting Mn and Mn/Ca species, compose the crystal structure of tiragalloite (Figure 1). Linkages among the ribbons are ensured by clusters of four vertex-sharing tetrahedra, three of which host Si atoms and the remaining hosting a mixed As/Si population. The vertex-sharing tetrahedral cluster originates a structural group of nominal composition $[\text{AsSi}_3\text{O}_{12}(\text{OH})]^{8-}$ that shares vertices also with octahedra centered at Mn(1), Mn(2) and Mn(4), and shares both vertices and edges with the 7-fold coordinated Mn(3) atom site.

It is worth noting that a short Mn(3)-T(3) non-bonding distance of $2.898(1) \text{ \AA}$ is detected between edge-sharing Mn(3)O₇ and T(3)(O₃OH). Such a distance is even shorter than the longest Mn(3)-O(7) bond distance, which is $2.939(2) \text{ \AA}$. Because the O-O edge shared between Mn(3)O₇ and T(3)(O₃OH) polyhedra is quite short, i.e. $2.509(2) \text{ \AA}$, any repulsive interaction between cations at Mn(3) and T(3) atom sites is shielded by these O-O edge. However, the Mn(3) site should be not suitable to host cations larger than Mn and, as shown in Table 3, the little Ca content is preferably located in the $^{[6]}\text{Mn}(4)(\text{O}_5\text{OH})$ octahedron, whose inter-cationic distances are larger than 3 \AA .

RESULTS AND DISCUSSION

The general organization of the crystal structure of tiragalloite as described by Gramaccioli et al. (1979) and Nagashima and Armbruster (2010) is confirmed by this work. The unit-cell volume of $1002.63(9) \text{ \AA}^3$ measured in this work is very close to that of $1002.49(3) \text{ \AA}^3$ measured by Nagashima and Armbruster (2010), and both are significantly smaller than that of $1012(2) \text{ \AA}^3$ reported by Gramaccioli et al. (1979). Such a high value derives from a reported c parameter of $7.67(1) \text{ \AA}$, to be compared with $7.5759(2) \text{ \AA}$ (this work) and $7.5750(1) \text{ \AA}$ (Nagashima and Armbruster, 2010). This in turn accounts for the larger volumes of the coordination polyhedra reported in Gramaccioli et al. (1979). However, the accuracy of the crystallographic data in Gramaccioli et al. (1979) is lower than in the present study and in the one of Nagashima and Armbruster (2010), as suggested by the reported e.s.d. and, for this reason, the relaxation of the structure reported by Gramaccioli et al. (1979) is not investigated.

On the contrary, the comparison between our data and those of Nagashima and Armbruster (2010) shows

Table 3. Refined site occupancies, atomic fractional coordinates and equivalent isotropic displacement parameters U_{eq} (\AA^2) for tiragalloite.

Site	Occupancy	x/a	y/b	z/c	U_{eq}
Mn(1)	1 Mn	0.25914(4)	0.64847(2)	-0.14605(4)	0.01127(5)
Mn(2)	1 Mn	-0.45779(4)	0.58383(2)	0.54598(4)	0.01121(5)
Mn(3)	0.972(6) Mn + 0.028(6) Ca	0.76325(4)	0.50880(2)	0.24555(4)	0.01274(6)
Mn(4)	0.940(6) Mn + 0.060(6) Ca	0.05278(4)	0.74592(2)	0.13914(4)	0.01155(6)
T(1)	1 Si	0.23132(7)	0.36792(3)	0.08053(6)	0.00875(7)
T(2)	1 Si	0.26718(7)	0.52069(3)	0.16133(6)	0.00851(7)
T(3)	1 Si	0.04811(7)	0.59790(3)	0.44020(6)	0.00886(8)
T(4)	0.925(2) As + 0.075(2) Si	0.43075(3)	0.30154(2)	-0.21219(2)	0.00896(5)
O(1)	1 O	0.2709(2)	0.23814(7)	-0.18170(19)	0.0128(2)
O(2)	1 O	0.4614(2)	0.32016(7)	-0.42049(18)	0.0138(2)
O(3)	1 O	0.6501(2)	0.28989(9)	-0.0898(2)	0.0163(2)
O(4)	1 O	0.3167(2)	0.37005(7)	-0.12197(17)	0.0118(2)
O(5)	1 O	0.0314(2)	0.32393(7)	0.07261(19)	0.0126(2)
O(6)	1 O	0.4157(2)	0.34325(7)	0.22044(18)	0.0116(2)
O(7)	1 O	0.1772(2)	0.44575(7)	0.1148(2)	0.0145(2)
O(8)	1 O	0.3016(2)	0.55369(7)	-0.02577(17)	0.0126(2)
O(9)	1 O	0.45893(19)	0.51565(7)	0.30833(17)	0.01108(19)
O(10)	1 O	0.0855(2)	0.55869(8)	0.25411(18)	0.0125(2)
O(11)	1 O	0.0508(2)	0.67828(7)	0.38331(19)	0.0154(2)
O(12)	1 O	0.22284(19)	0.58619(7)	0.60133(17)	0.01085(19)
O(13)	1 O	-0.1665(2)	0.56894(8)	0.47824(18)	0.0128(2)
H*	1 H	0.122(5)	0.7041(4)	0.479(2)	0.023**

* Atom coordinates refined with the soft restraint: O-H = 0.98 ± 0.01 \AA .

** constrained to be 1.5 time the U_{eq} of O(11) atom site.

peculiar features. Notwithstanding that the cell volume in our work is very close to that reported by Nagashima and Armbruster (2010) ($\Delta_{vol}=0.14$ \AA^3), there are small but significant differences in particular in the a and b cell parameters, with the a edge being 0.01 \AA shorter and the b edge 0.02 \AA longer in our study. These differences can be related to differences in the composition between the two crystals, having the tiragalloite of Nagashima and Armbruster (2010) a low amount of As (Table 1).

Table 6 reports the refined site occupancies and mean bond lengths from the two crystallographic studies for a comparison. In the refinement of Nagashima and Armbruster (2010), all Ca is located at the $^{[7]}\text{Mn}(3)\text{O}_7$ polyhedron, as occurs in medaite (a mineral studied in the same paper that hosts a little amount of Ca in a $^{[7]}\text{MnO}_7$ polyhedron), whereas As^{5+} and a little amount of V^{5+} are placed at the $^{[4]}\text{T}(4)\text{O}_4$ tetrahedron, together with a minor Si content.

Our study suggests a different ordering scheme for Ca, because the refined occupancies show that Ca is not hosted exclusively in the largest $^{[7]}\text{Mn}(3)\text{O}_7$ polyhedron,

but seems to prefer the $^{[6]}\text{Mn}(4)(\text{O}_5\text{OH})$ octahedron. As already mentioned, the Mn(3)-T(3) inter-cationic distance of $2.898(1)$ \AA can be the reason making the $^{[7]}\text{Mn}(3)\text{O}_7$ polyhedron not suitable to host the large Ca cation. Interestingly, in a recent study, Biagioni et al. (2019) show that in the crystal structure of arsenmedaite (isotypic with medaite) the minor Ca content is not all placed in the large seven-fold coordinated Mn(5) site but it results preferentially located in the six-fold coordinated Mn(6) site. Therefore, the distribution of Ca in the crystal structure of arsenmedaite is analogue to the one described in our study for tiragalloite.

As expected, the structure refinement confirms that As occupies the largest $^{[4]}\text{T}(4)\text{O}_4$ tetrahedron and the data reported in Table 6 show a larger difference of 0.007 \AA for the mean bond distances for the T(4) site, in agreement with the different amounts of As occurring at the $^{[4]}\text{T}(4)\text{O}_4$ tetrahedron. To sum up, the two structure refinements are in agreement for what concern the complete ordering of As atom at the $^{[4]}\text{T}(4)\text{O}_4$ tetrahedron, whereas they assume a different ordering for the minor Ca content. No

Table 4. Selected bond distances (Å), polyhedron volumes (Å³), polyhedral angle variances (°²), quadratic elongations, and mean square deviation from the average bond distances (Å²×10⁴) for tiragalloite.

Mn(1) site		Mn(2) site		Mn(3) site	
Mn(1)-O(1) ⁸	2.2107(15)	Mn(2)-O(2) ¹	2.1360(15)	Mn(3)-O(4) ²	2.6262(14)
Mn(1)-O(3) ²	2.2049(16)	Mn(2)-O(6) ⁴	2.2864 (14)	Mn(3)-O(7) ²	2.9395(16)
Mn(1)-O(5) ¹	2.1388(14)	Mn(2)-O(9) ⁵	2.2814(14)	Mn(3)-O(8) ²	2.0911(14)
Mn(1)-O(6) ²	2.2987(14)	Mn(2)-O(9') ⁴	2.2699(14)	Mn(3)-O(9)	2.1333(14)
Mn(1)-O(8)	2.1048(15)	Mn(2)-O(12) ⁵	2.2109(13)	Mn(3)-O(10) ³	2.3636(15)
Mn(1)-O(12) ⁹	2.2745(13)	Mn(2)-O(13)	2.0781(14)	Mn(3)-O(12) ⁶	2.2178(14)
				Mn(3)-O(13) ³	2.1460(15)
<Mn(1)-O>	2.2054	<Mn(2)-O>	2.2105	<Mn(3)-O>	2.3597
Volume	13.807(11)	Volume	13.912(11)	Volume	17.696(13)
OAV	86.19	OAV	76.29		-
OQE	1.025	OQE	1.025		-
Δ × 10 ⁴	9.612	Δ × 10 ⁴	12.760	Δ × 10 ⁴	152.989
Mn(4) site		T(1) site		T(2) site	
Mn(4)-O(1) ¹	2.2364(14)	T(1)-O(4)	1.6875(14)	T(2)-O(7)	1.6356(15)
Mn(4)-O(2) ⁸	2.2165(14)	T(1)-O(5)	1.5925(14)	T(2)-O(8)	1.5992(14)
Mn(4)-O(3) ²	2.1724(15)	T(1)-O(6)	1.6208(14)	T(2)-O(9)	1.6162(13)
Mn(4)-O(5)	2.1574(14)	T(1)-O(7)	1.6196(15)	T(2)-O(10)	1.6432(14)
Mn(4)-O(6) ⁷	2.2128(14)				
Mn(4)-O(11)	2.2901(15)	<T(1)-O>	1.6301	<T(2)-O>	1.6236
		Volume	2.209(3)	Volume	2.178(3)
<Mn(4)-O>	2.2142	TAV	18.35	TAV	24.21
Volume	13.914(11)	TQE	1.005	TQE	1.006
OAV	90.46	Δ × 10 ⁴	4.615	Δ × 10 ⁴	1.120
OQE	1.027				
Δ × 10 ⁴	3.824				
T(3) site		T(4) site			
T(3)-O(10)	1.6518(14)	T(4)-O(1)	1.6835(14)	O(11)-H	0.975(10)
T(3)-O(11)	1.6599(16)	T(4)-O(2)	1.6529(13)	H...O(1)	1.77
T(3)-O(12)	1.6215(14)	T(4)-O(3)	1.6712(14)	O(11)...O(1)	2.726(2)
T(3)-O(13)	1.5952(14)	T(4)-O(4)	1.7354(14)	<(O(11)-H...O(1))>	167.8°
<T(3)-O>	1.6321	<T(4)-O>	1.6858		
Volume	2.199(3)	Volume	2.441(3)		
TAV	38.06	TAV	20.53		
TQE	1.010	TQE	1.005		
Δ × 10 ⁴	2.468	Δ × 10 ⁴	3.309		

TAV=Tetrahedral Angle Variance; TQE=Tetrahedral Quadratic Elongation; OAV=Octahedral Angle Variance; OQE=Octahedral Quadratic Elongation were computed according to Robinson et al. (1971); Δ=mean square relative deviation from the average (Brown and Shannon, 1973).

Symmetry codes: ¹ -x, -y+1, -z; ² -x+1, -y+1, -z; ³ x+1, y, z; ⁴ -x, -y+1, -z+1; ⁵ x-1, y, z; ⁶ -x+1, -y+1, -z+1; ⁷ -x+½, y+½, -z+½; ⁸ -x+½, y+½, -z-½; ⁹ x, y, z-1.

information about the distribution of the Ca content can be extracted from the structure refinement performed by Gramaccioli et al. (1979), which have not refined the site populations.

For sake of clarity, the bond-valence analysis has been

performed and reported in Table 7. The analysis validates the results of the structure refinement because all bond valence sum for atom sites are within the 7% respect to theoretical values and the magnitude of the grand sum for all bonds (25.70 *vu* per formula unit) is very similar to the

Table 5. Anisotropic atomic displacement parameters (in Å²) for tiragalloite.

Site	U^{11}	U^{22}	U^{33}	U^{23}	U^{13}	U^{12}
Mn(1)	0.01181(10)	0.01086(11)	0.01116(10)	0.00035(7)	0.00128(7)	0.00068(7)
Mn(2)	0.01062(10)	0.01127(11)	0.01187(10)	0.00011(8)	0.00172(7)	0.00022(7)
Mn(3)	0.01201(11)	0.01405(12)	0.01216(10)	-0.00271(8)	0.00112(8)	-0.00232(8)
Mn(4)	0.01171(11)	0.01131(12)	0.01162(10)	-0.00130(8)	0.00108(8)	0.00006(8)
T(1)	0.00889(17)	0.00832(18)	0.00884(16)	-0.00004(13)	-0.00022(13)	-0.00074(13)
T(2)	0.00917(17)	0.00832(18)	0.00795(16)	0.00022(13)	0.00034(13)	0.00041(13)
T(3)	0.00843(17)	0.00949(19)	0.00853(16)	-0.00048(13)	0.00012(13)	0.00039(13)
T(4)	0.00922(7)	0.00962(8)	0.00798(7)	0.00056(5)	0.00058(5)	-0.00029(5)
O(1)	0.0133(5)	0.0099(5)	0.0156(5)	0.0001(4)	0.0037(4)	-0.0014(4)
O(2)	0.0218(6)	0.0113(5)	0.0088(5)	0.0003(4)	0.0042(4)	0.0010(4)
O(3)	0.0106(5)	0.0233(7)	0.0143(5)	-0.0021(5)	-0.0021(4)	0.0036(5)
O(4)	0.0142(5)	0.0117(5)	0.0099(5)	0.0002(4)	0.0028(4)	0.0006(4)
O(5)	0.0103(5)	0.0125(5)	0.0152(5)	-0.0016(4)	0.0022(4)	-0.0024(4)
O(6)	0.0109(5)	0.0137(5)	0.0098(5)	0.0009(4)	-0.0018(4)	0.0004(4)
O(7)	0.0139(5)	0.0098(5)	0.0193(6)	-0.0037(4)	-0.0009(4)	-0.0007(4)
O(8)	0.0156(5)	0.0127(5)	0.0096(5)	0.0010(4)	0.0014(4)	0.0000(4)
O(9)	0.0093(4)	0.0136(5)	0.0099(4)	0.0001(4)	-0.0008(3)	-0.0010(4)
O(10)	0.0114(5)	0.0151(6)	0.0111(5)	-0.0031(4)	0.0011(4)	0.0033(4)
O(11)	0.0219(6)	0.0107(6)	0.0130(5)	0.0007(4)	-0.0015(5)	0.0002(5)
O(12)	0.0105(5)	0.0123(5)	0.0094(4)	0.0000(4)	-0.0008(3)	0.0003(4)
O(13)	0.0097(5)	0.0156(6)	0.0133(5)	-0.0010(4)	0.0019(4)	-0.0007(4)

expected value (25.93 *vu* per formula unit).

The comparison of the chemical analyses of tiragalloite from different localities (Table 1) shows that there is a reasonable variability, in particular for the contents of As and Si. As it is known, a strong negative correlation occurs between Si and As and is due to the heterovalent $As^{5+} \leftrightarrow Si$ substitution (Nagashima and Armbruster, 2010). The chemical composition of tiragalloite from Scerscen results depleted in V_2O_5 with respect to the samples from the type locality and from Gambatesa (both Ligurian localities) and this should reflect the different origin of the samples. In fact, Ligurian tiragalloite was collected in Mn ore deposits embedded within metacherts belonging to the “Diaspri di Monte Alpe” formation; these rocks suffered metamorphic conditions estimated at $T=275 \pm 25$ °C, $P=0.25 \pm 0.05$ GPa by Cortesogno et al. (1979) and Lucchetti et al. (1990). On the contrary, tiragalloite studied in this work was found in manganese ore deposits belonging to sedimentary covers of the Margna Nappe in Valtellina, for which the metamorphism conditions were estimated at $T=420 \pm 30$ °C and $P=0.30 \pm 0.20$ GPa by Peters et al. (1978).

The different metamorphic grade in these localities can also affect the atom site populations detected in the crystals. The recalculated unit formula for the sample of this work is: $(Mn^{2+}_{3.86}Ca_{0.10})_{\Sigma 3.96}(As^{5+}_{0.85}V^{5+}_{0.02}Si_{0.19})_{\Sigma 1.06}Si_3O_{12}(OH)$,

whereas the unit formulae reported in literature are: $(Mn_{3.909}Ca_{0.077}Fe_{0.013})_{\Sigma 3.999}(As_{0.844}V_{0.116})_{\Sigma 0.960}Si_3O_{12}(OH)$, and $(Mn^{2+}_{3.85}Ca_{0.11}V^{3+}_{0.04})_{\Sigma 4.00}(As^{5+}_{0.64}Si_{0.32}V^{5+}_{0.04})_{\Sigma 1.00}Si_3O_{11.72}(OH)_{1.28}$ for the samples from the type locality (Gramaccioli et al., 1980) and from Gambatesa (Nagashima and Armbruster, 2010), respectively.

The sample studied in this work shows an As content of 0.85 a.p.f.u., with a significant degree of the heterovalent ($As^{5+} \leftrightarrow Si$) substitution and a small degree of the homovalent $As^{5+} \leftrightarrow V^{5+}$ substitution occurring at the T(4) site. A great amount of the heterovalent ($As^{5+} \leftrightarrow Si$) substitution was detected in the sample of Nagashima and Armbruster (2010), where the electrostatic balance is achieved using an excess of calculated OH from the stoichiometric value. On the contrary, a significant homovalent ($As^{5+} \leftrightarrow V^{5+}$) substitution was reported in the sample of Gramaccioli et al. (1980), whereas they did not take into consideration the $As^{5+} \leftrightarrow Si$ exchange, although an excess of Si was detected by chemical analysis.

As mentioned before, tiragalloite contains the $[AsSi_3O_{12}(OH)]^{8-}$ structural units characterized by one Si-OH silanol group and forms the 57.02 Dana's group together with hubeite, akatoreite, ruizite and cassagnaite. Hubeite, akatoreite, and ruizite contains four membered tetrahedral clusters populated only by Si atoms and

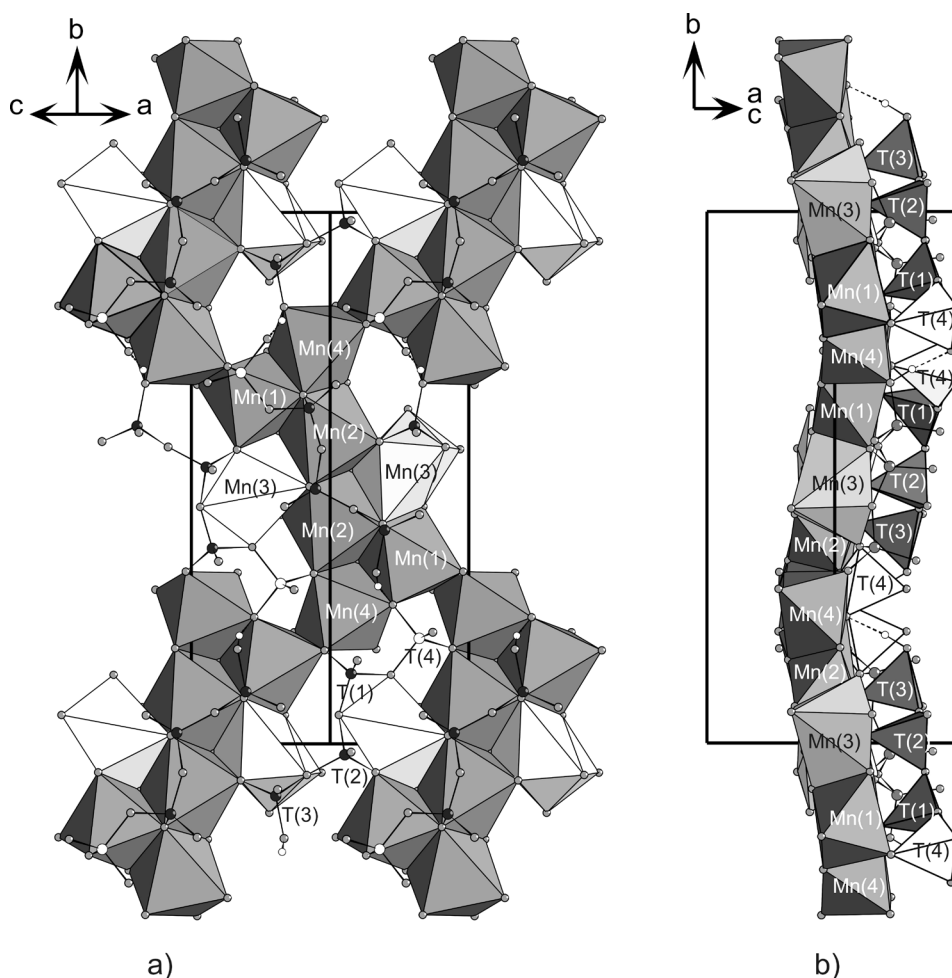


Figure 1. Crystal structure of tiragalloite showing the $^{[6]}\text{Mn}(1,2)\text{O}_6$ octahedra, the $^{[6]}\text{Mn}(4)(\text{O}_5\text{OH})$ octahedra, and the $^{[7]}\text{Mn}(3)\text{O}_7$ polyhedron forming the wavy ribbon together with the $[\text{AsSi}_3\text{O}_{12}(\text{OH})]^{8-}$ groups: (a) viewed along $[1\ 0\ 1]$ and (b) viewed along $[-1\ 0\ 1]$. To make the design of the structure clearer, some atoms have been omitted.

Table 6. Site occupancies and mean bond distances in tiragalloite. X=cation.

Site	This work		Nagashima and Armbruster (2010)	
	Assigned site-population (a.p.f.u.)	$\langle\text{X}-\text{O}\rangle$ (Å)	Assigned site-population (a.p.f.u.)	$\langle\text{X}-\text{O}\rangle$ (Å)
Mn(1)	1 Mn	2.205	1 Mn	2.208
Mn(2)	1 Mn	2.211	1 Mn	2.213
Mn(3)	0.972(6) Mn, 0.028(6) Ca	2.360	0.938(9) Mn, 0.062(9) Ca	2.359
Mn(4)	0.940(6) Mn, 0.060(6) Ca	2.214	1 Mn	2.218
T(1)	1 Si	1.630	1 Si	1.628
T(2)	1 Si	1.624	1 Si	1.620
T(3)	1 Si	1.632	1 Si	1.631
T(4)	0.925(2) As, 0.075(2) Si	1.686	0.700(3) As, 0.220(3) Si, 0.08 V	1.679

characterized by one (hubeite and akatoreite) or two (ruizite) Si-OH silanol groups, leading respectively to the formation of $[\text{Si}_4\text{O}_{12}(\text{OH})]^{9-}$ and $[\text{Si}_4\text{O}_{11}(\text{OH})_2]^{8-}$

structural units.

Arrangements of the four membered groups of tetrahedral and O-H...O linkages in presence of

Table 7. Bond valence analysis (ν) of tiragalloite.

Site charge	2.00	2.00	2.00	2.00	4.00	4.00	4.00	4.93	1.00	
Atom Site	Mn(1)	Mn(2)	Mn(3)	Mn(4)	T(1)	T(2)	T(3)	T(4)	H	
O(1)	0.32			0.31				1.22	0.24	2.09
O(2)		0.39		0.32				1.32		2.04
O(3)	0.33			0.37				1.26		1.96
O(4)			0.11		0.84			1.06		2.01
O(5)	0.39			0.38	1.10					1.87
O(6)	0.25	0.26		0.33	1.02					1.86
O(7)			0.05		1.02	0.97				2.04
O(8)	0.43		0.45			1.08				1.96
O(9)		0.27 0.28	0.40			1.03				1.98
O(10)			0.21			0.95	0.93			2.09
O(11)				0.27			0.92		0.76	1.95
O(12)	0.27	0.32	0.32				1.01			1.92
O(13)		0.46	0.39				1.09			1.94
Total	1.99	1.99	1.93	1.98	3.98	4.03	3.95	4.86	1.00	

Note: The valence of each site takes account of the contribution of different atom species; bond valence analysis calculated using bond-valence parameters from Brese and O'Keeffe (1991).

$[\text{AsSi}_3\text{O}_{12}(\text{OH})]^{8-}$, $[\text{Si}_4\text{O}_{12}(\text{OH})]^{9-}$ and $[\text{Si}_4\text{O}_{11}(\text{OH})_2]^{8-}$ structural units in these minerals are reported in Figure 2. Two different arrangements of the four membered groups of tetrahedra are present in these minerals: a linear conformation occurs in tiragalloite (Figure 2a), akatoreite (Figure 2b), and ruizite (Figure 2d) which is the only one containing two silanol groups, whereas a folded conformation originates in hubeite (Figure 2c). In tiragalloite, the silanol group is in a terminal position and linear $[\text{AsSi}_3\text{O}_{12}(\text{OH})]^{8-}$ structural units are linked to each other by hydrogen bonds forming an infinite chain extending along the b axis. In akatoreite as well, the silanol group is in a terminal position but two linear four membered tetrahedral units are linked to each other by two hydrogen bonds at the same end of the cluster, thus forming a linear $[\text{Si}_8\text{O}_{24}(\text{OH})_2]^{18-}$ dimer. In hubeite, the silanol group is in a terminal position of folded four membered tetrahedral clusters and two H-bonds connect two tetrahedral unit (related by an inversion center) forming an eight-membered ring of tetrahedra. In ruizite, the two silanol groups are placed at intermediate positions of the linear four membered tetrahedral cluster, and the hydrogen bond interactions define a sheet of tetrahedral clusters parallel to the (0 0 1) plane.

In addition to these minerals, the Si-OH silanol group occurs in the $\text{K}_5(\text{UO}_2)_2[\text{Si}_4\text{O}_{12}(\text{OH})]$ synthetic compound (Chen et al., 2005), the first synthesized uranium silicate phase that contains finite linear chains of four tetrahedra

arranged in $[\text{Si}_4\text{O}_{12}(\text{OH})]^{9-}$ structural units. As in tiragalloite, the silanol group is in a terminal position and the adjacent four-membered groups of Si-populated tetrahedra are linked by hydrogen bonds forming chains along the b axis.

On the contrary, several synthetic phases are characterized by the tetrasilicate $(\text{Si}_4\text{O}_{13})^{10-}$ groups, a structural motif still unknown in minerals. Some of these compounds are: $\text{Ba}_2\text{Gd}_2(\text{Si}_4\text{O}_{13})$ (Wierzbicka-Wieczorek et al., 2010), $\text{Ag}_{10}(\text{Si}_4\text{O}_{13})$ (Jansen and Keller, 1979), $\text{Na}_4\text{Sc}_2(\text{Si}_4\text{O}_{13})$ (Maksimov et al., 1980), $\text{Ba}_2\text{Nd}_2(\text{Si}_4\text{O}_{13})$ (Tamazyan and Malinovskii, 1985), $\text{K}_5\text{Eu}_2\text{F}(\text{Si}_4\text{O}_{13})$ (Chiang et al., 2007), $\text{Ag}_{18}(\text{SiO}_4)_2(\text{Si}_4\text{O}_{13})$ (Heidebrecht and Jansen, 1991), and $\text{La}_6(\text{Si}_4\text{O}_{13})(\text{SiO}_4)_2$ (Müller-Bunz and Schleid, 2002). The first five phases show finite tetrasilicate groups characterized by zigzag shape, whereas $\text{Ag}_{18}(\text{SiO}_4)_2(\text{Si}_4\text{O}_{13})$ and $\text{La}_6(\text{Si}_4\text{O}_{13})(\text{SiO}_4)_2$ phases, that contain also additional isolated $(\text{SiO}_4)^{4-}$ groups, show a stretched zigzag configuration and a horseshoe-shaped Si_4O_{13} unit, respectively (Wierzbicka-Wieczorek et al., 2010).

These synthetic phases characterized by four interconnected Si populated tetrahedra without the silanol group (structural motif still unknown in minerals) show the Si-O_{br}-Si bond angles in the range 123-148° (131-149° for $\text{K}_5(\text{UO}_2)_2[\text{Si}_4\text{O}_{12}(\text{OH})]$). Similar values for angles involving the bridging oxygens are observed also in mineral of the tiragalloite group. In particular, for Si populated tetrahedra,

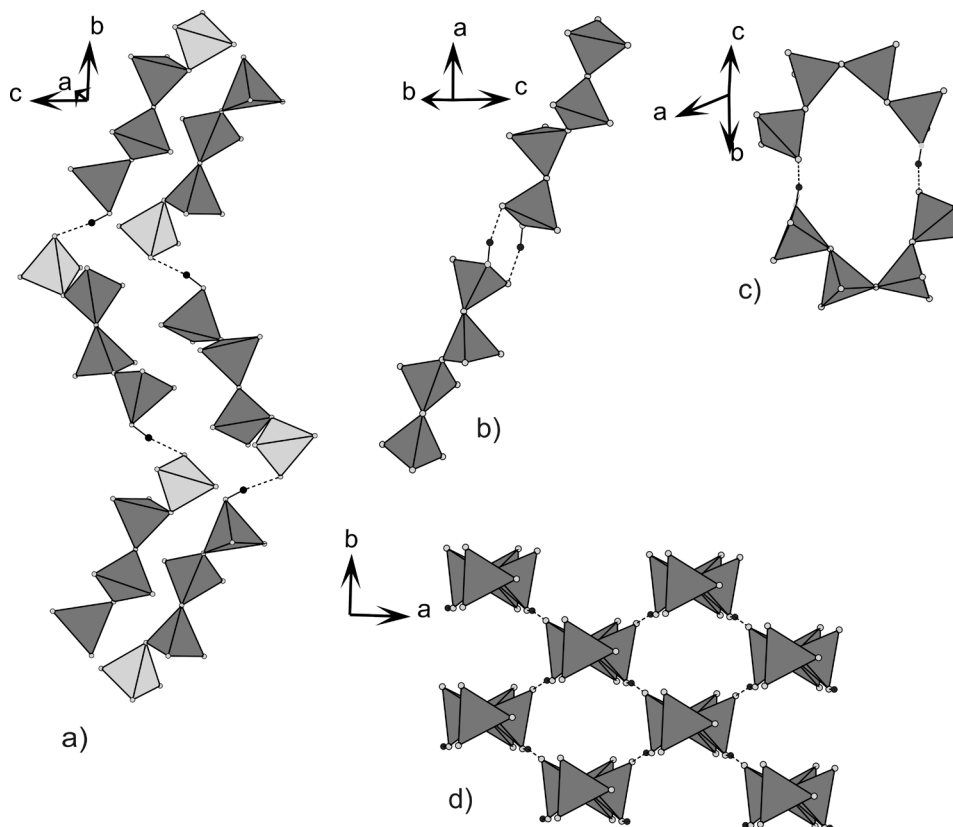


Figure 2. The arrangement of the four membered groups of tetrahedra in (a) tiragalloite; (b) akatoreite; (c) hubeite; (d) ruizite.

the Si-O_{br}-Si bond angles are in the range 128-167° whereas in presence of the As populated tetrahedron of tiragalloite, the As-O_{br}-Si angle decreases to 122°.

ACKNOWLEDGEMENTS

The tiragalloite sample used in this work was donated to the Mineralogical Museum of the University of Pavia by the collector Franco Benetti, who is warmly thanked. The “Laboratorio Arvedi” of the University of Pavia and Maria Pia Riccardi are acknowledged for allowing the use of the electron microscope. Thanks are also due to Andrea Risplendente of the University of Milan for his supporting in the microchemical analysis. The authors wish to thank the Editor Alessandro Pacella for handling the review process efficiently and the anonymous referee for the constructive comments. This work was supported by the Ministero dell’Istruzione, dell’Università e della Ricerca and by the University of Pavia.

REFERENCES

Abrecht J., 1990. An As-rich manganiferous mineral assemblage from the Ködnitz Valley (Eastern Alps, Austria): geology, mineralogy, genetic considerations, and implications for metamorphic Mn deposits. *Neues Jahrbuch für Mineralogie*,

Monatshefte 8, 363-375.

Biagioni C., Belmonte D., Carbone C., Cabella R., Zaccarini F., Balestra C., 2019. Arsenmedaite, Mn₆²⁺As⁵⁺Si₅O₁₈(OH), the arsenic analogue of medaite, from the Molinello mine, Liguria, Italy: occurrence and crystal structure. *European Journal of Mineralogy* 31, 117-126.

Blessing R.H., 1995. An empirical correction for absorption anisotropy. *Acta Crystallographica Section A* 51, 33-38.

Breese N.E. and O’Keeffe M., 1991. Bond-valence parameters for solids. *Acta Crystallographica B* 47, 192-7.

Brown I.D. and Shannon R.D., 1973. Empirical bond-strength-bond-length curves for oxides. *Acta Crystallographica A* 29, 266-282.

Brugger J., Krivovichev S., Meisser N., Ansermet S., Armbruster T., 2006. Scheuchzerite, Na(Mn,Mg)₉[VSi₉O₂₈(OH)](OH)₃, a new single-chain silicate. *American Mineralogist* 91, 937-943.

Bruker, 2003. SAINT Software reference manual, version 6. Bruker AXS Inc., Madison, Wisconsin, USA.

Callegari A., Sciesa F., Bedogné F., 1992. Primo ritrovamento di tiragalloite Mn₄[AsSi₃O₁₂(OH)] in Val Malenco (Sondrio Italia settentrionale). *Il naturalista Valtellinese* 3, 3-9.

Cámara F., Bittarello E., Ciriotti M.E., Nestola F., Radica F., Marchesini M., 2015. As-bearing new mineral species from

- Valletta mine, Maira Valley, Piedmont, Italy: II. Braccoite, $\text{NaMn}^{2+}_5[\text{Si}_5\text{AsO}_{17}(\text{OH})](\text{OH})$, description and crystal structure. *Mineralogical Magazine* 79, 171-189.
- Cenki-Tok B. and Chopin C., 2006. Coexisting calderite and spessartine garnets in eclogite-facies metacherts of the Western Alps. *Mineralogy and Petrology* 88, 47-68.
- Chen C.-S., Kao H.-M., Lii K.-H., 2005. $\text{K}_5(\text{UO}_2)_2[\text{Si}_4\text{O}_{12}(\text{OH})]$: A uranyl silicate containing chains of four silicate tetrahedra linked by $\text{SiO}\cdots\text{HOSi}$ hydrogen bonds. *Inorganic Chemistry* 44, 935-940.
- Chiang P.-Y., Lin T.-W., Dai J.-H., Chang B.-C., Kwang-Hwa Lii K.-H., 2007. Flux Synthesis, Crystal Structure, and Luminescence Properties of a New Europium Fluoride-Silicate: $\text{K}_5\text{Eu}_2\text{FSi}_4\text{O}_{13}$. *Inorganic Chemistry* 46, 3619-3622.
- Clark A., 1993. *Hey's Chemical Index of Minerals*. Third edition. Published by Chapman and Hall, London. ISBN 978-0-412-39950-3.
- Cortesogno L., Lucchetti G., Penco A.M., 1979. Le mineralizzazioni a manganese nei diaspri delle ofioliti liguri: mineralogia e genesi. *Rendiconti S.I.M.P.* 35, 151-197.
- Franks F., 1973. *Water: a comprehensive treatise*, 2. Plenum, New York, 684 pp.
- Gaines R.V., Skinner H.C.W., Foord E.E., Mason B., Rosenzweig A., 1997. *Dana's New Mineralogy*. Eighth Edition. New York and Chichester (John Wiley and Sons, Ltd.). ISBN 0-471-19310-0.
- Gramaccioli C.M., Pilati T., Liborio G., 1979. Structure of a manganese (II) arsenatotrisilicate, $\text{Mn}_4[\text{AsSi}_3\text{O}_{12}(\text{OH})]$: the presence of a new tetrapolyphosphate-like anion. *Acta Crystallographica B* 35, 2287-2291.
- Gramaccioli C.M., Griffin W.L., Mottana A., 1980. Tiragalloite, $\text{Mn}_4[\text{AsSi}_3\text{O}_{12}(\text{OH})]$, a new mineral and the first example of arsenatotrisilicate. *American Mineralogist* 65, 947-952.
- Heidebrecht K. and Jansen M., 1991. $\text{Ag}_{18}(\text{SiO}_4)_2(\text{Si}_4\text{O}_{13})$, das erste Silbersilicat mit gemischten Anionen. *Zeitschrift für anorganische und allgemeine Chemie* 597, 79-86.
- Ibers J.A. and Hamilton W.C., 1992. *International Tables for X-ray Crystallography*, Vol. C. Dordrecht: D. Reidel Publishing.
- Jansen M. and Keller H.L., 1979. $\text{Ag}_{10}\text{Si}_4\text{O}_{13}$, das erste Tetrasilicat. *Angewandte Chemie* 91, 500.
- Lucchetti G., Cabella R., Cortesogno L., 1990. Pumpellyite and coexisting minerals in different low grade metamorphic facies of Liguria, Italy. *Journal of Metamorphic Geology* 8, 539-550.
- Maksimov B.A., Melnikov O.K., Zhdanova T.A., Ilyukhin V.V., Belov N.V., 1980. Crystal structure of $\text{Na}_4\text{Sc}_2\text{Si}_4\text{O}_{13}$. *Doklady Akademii Nauk SSSR*, 251, 98-102.
- Müller-Bunz H. and Schleid T., 2002. $\text{La}_2\text{Si}_2\text{O}_7$ im I-Typ: Gemäß $\text{La}_6[\text{Si}_4\text{O}_{13}][\text{SiO}_4]_2$ kein echtes Lanthandisilicat. *Zeitschrift für anorganische und allgemeine Chemie* 628, 564-569.
- Nakao T., Fujiwara T., Matsubara S., Miyawaki R., 2005. Tiragalloite from the Yamato mine, Amami- Ohshima Island, Kagoshima Prefecture, Japan. Abstract for Annual Meeting of the Mineralogical Society of Japan 129. (in Japanese with English abstract).
- Nagashima M. and Armbruster T., 2010. Ardenite, tiragalloite and medaite: structural control of $(\text{As}^{5+}, \text{V}^{5+}, \text{Si}^{4+})\text{O}_4$ tetrahedra in silicates. *Mineralogical Magazine* 74, 55-71.
- Niedermayr V.G., Auer C., Bernhard F., Bojar H.P., Brandstätter F., Grill J., Gröbner J., Hollerer C.E., Knobloch G., Kolitsch U., Lamatsch P., Löffler E., Pieler E., Postl W., Prasnik H., Schachinger T., Schillhammer H., Taucher J., Wa F., 2015. Neue mineralfunde aus Österreich LIX. *Carinthia II*, 205./125., 207-280.
- Peters Tj., Trommsdorff V., Sommerauer J., 1978. Manganese pyroxenoids and carbonates: critical phase relations in metamorphic assemblages from the Alps. *Contributions to Mineralogy and Petrology* 66, 383-388.
- Piccoli G.C., Maletto G., Bosio P., Lombardo B., 2007. Minerali del Piemonte e della Valle d'Aosta. Associazione Amici del Museo "F. Eusebio" Alba, Ed., Alba (Cuneo) 607 pp.
- Roth P. and Meisser N., 2011. I minerali dell'Alpe Tanatz. Passo dello Spluga (Grigioni, Svizzera). *Rivista Mineralogica Italiana* 2, 90-99.
- Robinson K., Gibbs G.V., Ribbe P.H., 1971. Quadratic elongation, a quantitative measure of distortion in coordination polyhedra. *Science* 172, 567-570.
- Sheldrick G.M., 2003. SADABS. University of Göttingen, Germany.
- Sheldrick G.M., 2015. Crystal structure refinement with SHELXL. *Acta Crystallographica C* 71, 3-8.
- Tamazyan R.A. and Malinovskii Yu. A., 1985. Crystal structure of $\text{Nd}_2\text{Ba}_2[\text{Si}_4\text{O}_{13}]$. *Doklady Akademii Nauk SSSR*, 285, 124-183.
- Wierzbicka-Wieczorek M., Kolitsch U., Tillmanns E., 2010. $\text{Ba}_2\text{Gd}_2(\text{Si}_4\text{O}_{13})$: a silicate with finite Si_4O_{13} chains. *Acta Crystallographica C* 66, i29-i32.



This work is licensed under a Creative Commons Attribution 4.0 International License CC BY. To view a copy of this license, visit <http://creativecommons.org/licenses/by/4.0/>

